EFDA–JET–CP(09)06/34

D. Van Eester, E. Lerche, A. Argouarch, T. Blackman, F. Durodie, M. Evrard,
R.H. Goulding, S. Huygen, P. Jacquet, M.-L. Mayoral, I. Monakhov,
M. Nightingale, J. Ongena, M. Vrancken, E. Wooldridge, A. Whitehurst
and JET EFDA contributors

Numerical Tools for Monitoring the ITER-like Antenna at JET

Numerical Tools for Monitoring the ITER-like Antenna at JET

D. Van Eester[1], E. Lerche[1], A. Argouarch[2], T. Blackman[3], F. Durodie[1], M. Evrard[1], R.H. Goulding[4], S. Huygen[1], P. Jacquet[3], M.-L. Mayoral[3], I. Monakhov[3], M. Nightingale[3], J. Ongena[1], M. Vrancken[1], E. Wooldridge[3], A. Whitehurst[3] and JET EFDA contributors*

JET-EFDA, Culham Science Centre, OX14 3DB, Abingdon, UK

[1]Association EURATOM-Belgian State, Koninklijke Militaire School - Ecole Royale Militaire, B-1000 Brussels Belgium
[2]EURATOM/CEA, CEA/DSM/DRFC, F-13108, St.-Paul-lez-Durance , France
[3]EURATOM-UKAEA Fusion Association, Culham Science Centre, OX14 3DB, Abingdon, OXON, UK
[4]ORNL, P.O. Box 20008, MS-6169, Oak Ridge, Tennessee, TN 37831-6169, United States
** See annex of F. Romanelli et al, "Overview of JET Results",*
(Proc. 22 nd IAEA Fusion Energy Conference, Geneva, Switzerland (2008)).

Preprint of Paper to be submitted for publication in Proceedings of the
36th EPS Conference on Plasma Physics, Sofia, Bulgaria.
(29th June 2009 - 3rd July 2009)

1. INTRODUCTION

A new Ion Cyclotron Resonance Frequency (ICRF) antenna referred to as the 'ITER-Like Antenna' (ILA) is currently being tested at JET [1]. The ILA has been designed to achieve power densities similar to those required for ITER and to cope with the fast variations in coupling conditions due to ELMs, characteristic for the high confinement regime in which ITER will mainly be operated. The ILA consists of 8 short antenna straps, linked in a T-junction con- figuration to 4 (30Ω) coaxial transmission lines going to the generator. The plasma in front of the antenna acts as a varying load. In order to minimize the reflected power that comes back along the transmission lines, several elements at different locations on the lines can be adjusted, in particular the values of 8 capacitors situated just behind the straps and of 8 RF mechanical elements (1 stub and 1 phase shifter per resonant double loop or RDL; see Fig.1). As the 4 RDLs are coupled, any change on one of the tuning elements affects the required settings of all the other elements. Some adjustments are made in real-time based on reflected and forward voltage measurements but in order to further optimize the different settings and understand the experimental results better, the ILA simulator - a modeling tool based on the theory of Radio-Frequency (RF) wave propagation in a transmission line and on the RF model of the ILA circuit [2] - was developed in order to model the voltage and current at various places in the ILA circuit.

2. TELEGRAPHER'S EQUATIONS

Capturing the full dynamics of the electromagnetic waves in the antenna system requires solving Maxwell's equations. Because of the complicated geometry of the system, this would require excessive CPU time and memory. Hence, counting on such sophisticated tools would prohibit having a good understanding of the wave pattern on a shot-to-shot basis. Luckily, the telegrapher's equations - simplified equations retaining only the dominant transmission line mode - suffice to get an image of the wave dynamics in the circuit. A series of MicroWave Studio runs [2] has been performed and has provided the equivalent electrical lengths and characteristic impedances of the various ILA circuit elements needed in these equations. The telegrapher's equations are $dV/dx = Z_L I$ and $dI/dx = -Y_L V$, in which Z_L is the impedance and Y_L is the admittance of the transmission line per unit length. They link the voltage V and the current I and admit a forward and a backward propagating solution: $V(x)=V_+ + V_- = V_+(x_o)exp(-\zeta) + V(x_o)exp(+\zeta)$, $I(x) = [V_+ + V_-]=Z_o$, *in which* $\zeta = \gamma(x-x_o)$, $\gamma = (Z_L Y_L)^{1/2}$ is the propagation constant and $Z_o = (Z_L/Y_L)^{1/2}$ is the characteristic line impedance. This solution can be cast in matrix form, linking voltages and currents at neighboring locations: $(V,I)_{xm} = \bar{\bar{\boldsymbol{B}}}_{mn}.(V, I)x_n$. To propagate the solutions along transmission line segments with different Z_o and lengths, it suffices to 'click' the various matrices $\boldsymbol{B}$ together: $(V,I)_{end} = \bar{\bar{\boldsymbol{B}}}....\bar{\bar{\boldsymbol{B}}}....\bar{\bar{\boldsymbol{B}}}_{01}.(V, I)_{start}$.

3. SCATTERING MATRIX ARC DETECTION

High power operation requires high voltages at the straps and in the transmission lines and may cause arcing. Since this arcing not only causes malfunctioning of the antenna as it unmatches the system but - more dangerously - may damage the system because of the intense local energy dissipation associated with it, arc detection is instrumental. Commonly, it relies on the measurement of the voltage standing wave ratio (VSWR= $[1+|\Gamma|]/[1-|\Gamma|]$, in which Γ is the reflection coefficient) at a given point of the transmission lines feeding the antennae. Since they do not cause big changes of the VSWR, arcs that occur at low impedance locations, however, go unnoticed by this traditional technique. The ILA - which has a low impedance T-point - is vulnerable in that respect. Hence a more sophisticated arc detection system was required. ILA's Scattering Matrix Arc Detection (SMAD) [2] has shown to meet this requirement [3]. Basically, SMAD performs a consistency check between 4 measured voltages around the T-junction: the forward'V_{+APTL}'and reflected V_{-APTL} voltages at the APTL (Antenna Pressurized Transmission Line) feeding point and the voltages V_U and V_L close to the antenna straps. Given the 3×3 scattering matrix $\bar{\bar{\mathbf{S}}}$ for the T-junction (obtained from MWS modeling or from the equivalent RF model [2]), one can indeed explicitly write down 3 linear relations binding the 4 measured quantities and the 2 non-measured currents flowing between the capacitors and the antenna straps: $I_U = \alpha_{UU} V_U + \alpha_{UL} V_L + \alpha_U V_{+APTL}$, $IL = \alpha_{LU} V_U + \alpha_{LL} V_L + \alpha_L V_{+APTL}$, $V_{-APTL} = \zeta_U V_U + \zeta_L V_L + \zeta V_{+APTL}$, the coefficients in which depend on the components of $\bar{\bar{S}}$ and the capacitor values. The latter of these equations is used for detecting arcs.

4. THE ILA CIRCUIT SIMULATOR

Using the 8×8 impedance matrix linking strap voltages to strap currents [4], the 3ξ3 scattering equations across the T-junctions [2, 3], the $\bar{\bar{\boldsymbol{B}}}$ matrices for propagating solutions along the transmission lines, and - if needed - the 4-point junction coupling matrices representing the 3dB combiners (which were present at the outset of the ILA commissioning) one can write down the basic equations governing the complete ILA circuit. The ILA simulator solves this (linear) system, i.e. provides the voltages and currents consistent with given settings of the tuning elements at key points in the circuit. The ILA simulator can be run in 2 modes: Either the values of the various tuning elements are assumed to be known. Alternatively, some of these settings are assumed to be known only approximately, in which case their actual values can be determined using a minimization procedure that implements the simulator as a subroutine. Various minimization strategies can be opted for: finding the capacitor settings for a given experimental Z_T, finding the circuit element settings that ensure the actual phasing at the straps, Figure 2 shows an example of the ILA simulator's output for 42MHz L-mode Pulse No: 75329 for which P_{ILA} = 4.2MW.

On top of it giving a possibility to correct for unavoidable measuring errors, the main interest of the minimizer is that it allows to explore the available parameter domain to come up with settings for the matching elements, a second stage setter being the key application.

CONCLUSIONS

A transmission line model tool has been developed to monitor and predict the voltages and currents in the ILA circuit. It allows to perform consistency checks on the data and to determine the sensitiveness of the standing wave pattern in the lines to isolated or combined modifications of the tuning elements. It can be operated in a predictive or an interpretative mode, either using given (commonly experimentally read) data or adopting a minimization procedure to correct for unavoidable inaccuracies of the measurements. The ILA simulator has been used to crosscheck and provide the coefficients of the SMAD system, to identify calibration inaccuracies and to adjust second stage settings both in L- and H-mode operation.

ACKNOWLEDGEMENT

This work, supported by the European Communities under the contract of the Association between EURATOM and the Belgian State, was carried out within the framework of the European Fusion Development Agreement. The views and opinions expressed herein do not necessarily reflect those of the European Commission.

REFERENCES

[1]. F. Durodie, Ph. Chappuis, J. Fanthome, R.H. Goulding, J. Hosea, P.U. Lamalle, et al., Fusion Engineering and Design **74** (2005) 223-228.

[2]. M. Vrancken *et al.*, Scattering-Matrix Arc Detection on the JET ITER-Like ICRH Antenna, SOFT-2008; in press in Fusion Engineering and Design (FUSION-4583).

[3]. M. Vrancken *et al.*, Operational Experience with the Scattering Matrix Arc Detection on the JET ITER-like Antenna, 18th Topical Conference on Radio Frequency Power in Plasmas, Ghent, 2009.

[4]. M. Vrancken *et al.*, Proc. 17th Topical Conference on Radio Frequency Power in Plasmas, AIP Conference Proceedings **933**, Clearwater, 2007, pp. 131-134.

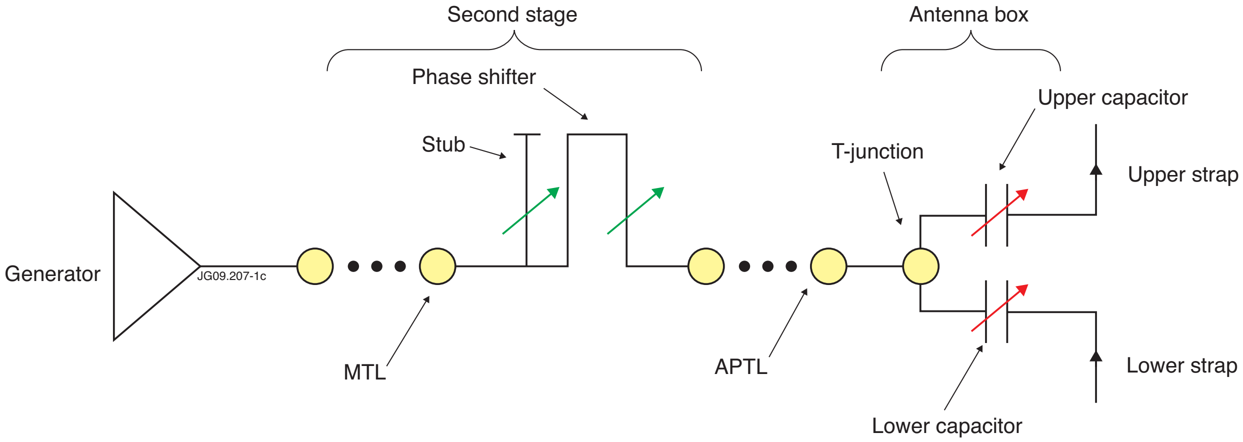

Figure 1: Schematic drawing of 1 of the 4 ILA RDLs, indicating the variable elements used for tuning the circuit.

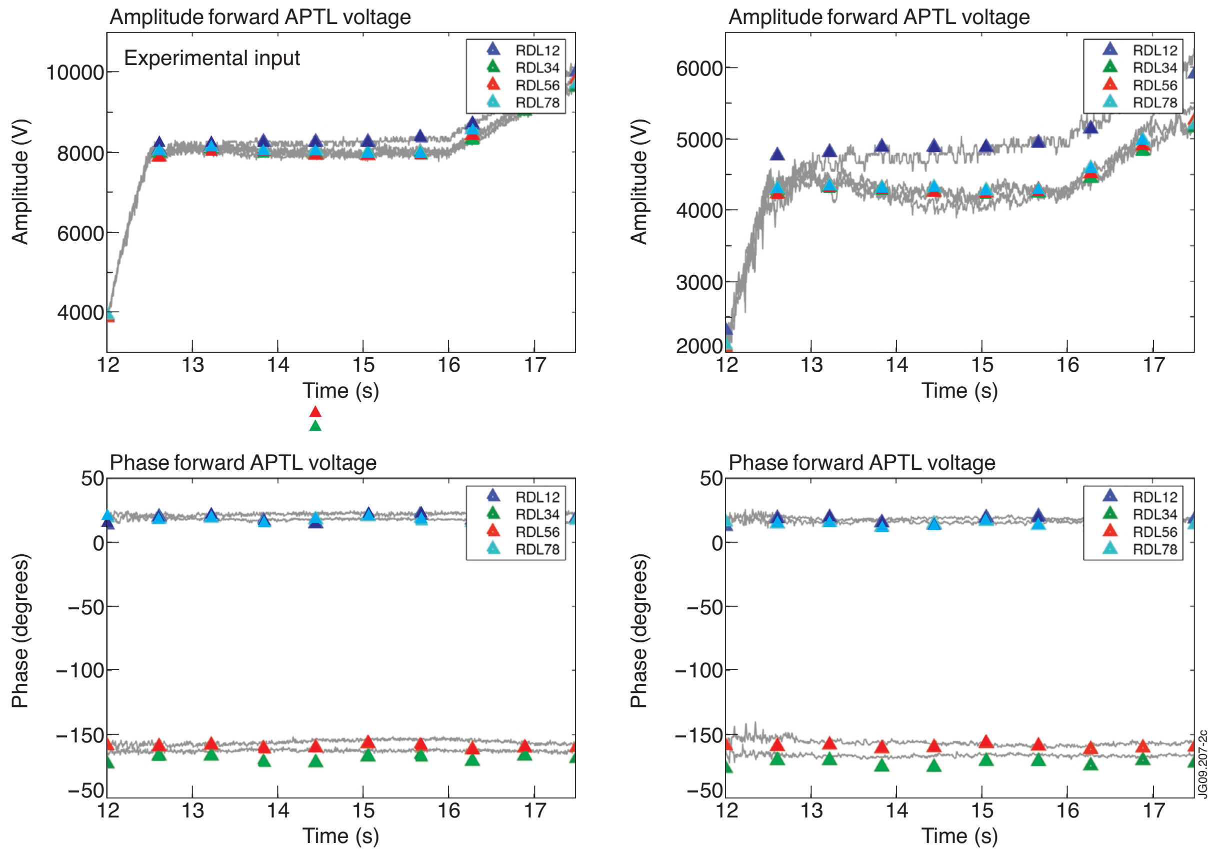

Figure 2: Amplitude (top) and phase (bottom) of the forward (left) and reflected (right) voltages at the APTL for Pulse No: 75329. Symbols are simulated data; full lines are measured data. The top left data is assumed known while the other data is output. The APTL phases are slightly changed by the minimizer to ensure having the proper experimental phases at the straps.